Electronic Supplementary Sheet for

ATP foster tuning of Nanostructured CeO_2 Peroxidase-like activity for promising Anti-bacterial performance

Benazir Chishti[1], H. Fouad[2,3*], H. K. Seo[4], Othman Y. Alothman[5], Z.A. Ansari[1], S. G. Ansari[1]*

[1]Centre for Interdisciplinary Research in Basic Science, Jamia Millia Islamia, New Delhi 110025, India

[2]Applied Medical Science Dept. Community College, King Saud University, P.O Box 10219, Riyadh 11433, Saudi Arabia

[3]Biomedical Engineering Department, Faculty of Engineering, Helwan University, Helwan, 11792, Egypt

[4]School of Chemical Engineering, Jeonbuk National University, Jeonju 54896, South Korea

[5]Chemical Engineering Department, College of Engineering, King Saud University, Riyadh, Saudi Arabia

*Corresponding Authors: S.G. Ansari (saansari@jmi.ac.in),
H. Fouad (menhfefnew@hotmail.com)

Outline: Supporting information includes tabulated scheme discussing the present limitations, issues addressed in the manuscript and following sections, figures, and Tables:

ESS Sections:

ESS 1.1 Synthetic protocol for preparing catalysts (CeO_2 NCs).

ESS 1.2 XPS analysis to identify % Ce^{3+} and Ce^{4+} concentration in CeO_2 NCs.

ESS 1.3 Optimization of Peroxidase (POD) assay parameters.

ESS 1.4 Influence of pH on catalyst POD reaction; role of ATP.

ESS 1.5 Fluorometric Resazurin Microplate assay (f-REMA).

ESS 1.6 Minimum Inhibitory Concentration (MIC).

ESS 1.7 Influence of H_2O_2 on bacterial growth (at pH 4.5 & 7.4).

ESS Figures:

S1 Deconvoluted XPS spectra of Ce (3d) region

S2 Optimization of substrate (TMB & H_2O_2) concentration for POD-like-activity in CeO_2 NCs. at pH 4.5.

S3 Schematic illustration of catalyst (CeO_2 NCs.)-catalyzed oxidation of TMB and typical photography of TMB-H_2O_2 reaction system.

S4 Substrate concentration dependent POD-like activity of CeO_2 NCs. at pH 4.5 & 7.4 for **(a)** TMB 0.1-0.6 mM; **(b)** H_2O_2 1-5 mM.

S5 Steady-state kinetic assay of CeO_2 NCs. at pH 4.5 (**a)** 3.5 mM of H_2O_2 with different concentrations of TMB (0.1-0.6 mM); **(b)** 0.3 mM of TMB mM with different concentrations of H_2O_2 (1-5 mM). Double reciprocal given as inset.

S6 Steady-state kinetic assay of CeO_2 NCs. at pH 7.4 **(a)** 3.5 mM of H_2O_2 with different concentrations of TMB (0.1-0.6 mM); **(b)** 0.3 mM of TMB mM with different concentrations of H_2O_2 (1-5 mM). Double reciprocal given as inset.

S7 Effect of incubation time on the absorbance of TMB-H_2O_2 reaction catalysed by CeO_2 NCs. at **(a)** pH 4.5 & **(b)** 7.4.

S8 (a) Influence of pH on formation of oxidised TMB and **(b)** heat map for (%) Relative activity at pH 4.5 & 7.4.

S9 (a) Effect of adenosine analogues (AMP, ADP and ATP) and histidine on the TMB-H_2O_2 reaction catalysed by CeO_2 NCs. in PBS (1X) at pH 7.4. **(b)** Effect of adenosine analogues

(AMP, ADP, ATP) and histidine in stabilizing cation radical ($TMB^{\cdot+}$) at neutral pH (7.4); inset shows the related color reactions after 60 minutes.

S10 Reusability Experiment: POD-like-activity in CeO_2 NCs. after every cycle at **(a)** pH 4.5; **(b)** pH 7.4.

S11 XRD pattern of CeO_2 NCs. post synthesis and recovered after 10 catalytic cycles performed at pH 4.5 and 7.4.

S12 Fluorescence spectra of 2- hydroxy terephthalic acid for detection of hydroxyl radical (•OH) using terephthalic acid (TA) as probe.

S13 Calibration curve for **(a)** *S. aureus* **(b)** *E. coli.*

S14 (a) Bacterial Survival (%) verses oxidant (H_2O_2) concentrations; **(b)** LP in oxidant (H_2O_2) treated bacterial cells; **(c)** Catalyst substrate (H_2O_2) dependent POD activity, inset shows •OH radical generation using TA probe at pH 4.5 and 7.5.

ESS Table

Table S1 Binding energies and Peak areas for Ce^{3+} and Ce^{4+} ion concentration

Table S2 Catalyst $MIC_{99\%}$ ($\mu g\ mL^{-1}$) alone and in combination

Table S3 Comparative Assessment of CeO_2 NCs. Anti-bacterial potential with earlier reports

Limitations of the present POD mimic addressed

Limitations/Challenges	Issues address in this manuscript
Catalytic activity within narrow pH range.	POD-mimic activity in ATP-CeO_2 NCs shows broad pH scope (3-8) with maximum activity at neutral pH (7.4).
Clinically use concentration of H_2O_2 (traditional bactericide) inhibits wound healing and damages normal tissues.	Catalyst exhibits low K_m for H_2O_2; reduces the effective concentration to ~285 times promoting anti-bacterial performance of H_2O_2 and cause no harm to normal tissues at low doses.
Antibiotic-resistant bacterial strains	POD-mimic nanozyme (CeO_2 NCs.) catalyse low dose H_2O_2 transformation into •OH radicals which helps to combat bacterial growth.

1.1 Material synthesis

CeO_2 NCs. were synthesized using co-precipitation method. In a typical reaction, 24 mg $CeCl_3 \cdot 7H_2O$ was dissolved in 20 mL DI water and magnetically stirred for 1 hr to obtain homogenous solution of 7 mM. 25% (W/V) ammonia (NH_3) solution was added drop wise under continuous stirring to achieve pH 10.5 followed by heating at 60ºC in water bath for 1 hr to promote deprotonation of product before precipitation. The solution was stirred for 22 hrs at room temperature to obtain the uniform growth distribution. White precipitate was washed several times with DI water to remove excess ions and unreacted salts; confirmed from solution pH 7.2; followed by drying in an oven at 70ºC gives ceria NCs. The characterization and other assays were performed at room temperature and pressure unless and otherwise mentioned.

1.2 XPS Analysis

Gaussian fitting applied to Ce (3d) spectrum and analysed for the deconvoluted peaks. These multiple peaks arise from mixed valence state (+3 and +4) in cerium as well as due to multiple d-splitting. Ten deconvoluted peaks show in Fig. S1 was used to calculate % of Ce^{3+} and Ce^{4+} ion concentration using integrated area under curve in the following equation (i & ii): [1]

$$\left[\%Ce^{3+}\right] = \frac{Av_o + Av' + Au_o + Au'}{\Sigma A_i} \quad \text{Equation (i)}$$

$$\left[\%Ce^{4+}\right] = \frac{Av + Av'' + Av''' + Au + Au'' + Au'''}{\Sigma A_i} \quad \text{Equation (ii)}$$

Where, $Av_o, Av', Au_o, Au', Av, Av'', Av'''$, Au, Au'' and Au''' are areas of the respective band given in Table S1; A_i= Integrated peak areas

Table S1 Binding energies and Peak areas for Ce^{3+} and Ce^{4+} ion concentration

Sample	Peak Assignment	Binding energy (eV)	Ce contribution (+3/+4)	Peak Area
CeO_2	u	900.4	+4	22179.10
	u_o	899.01	+3	17732.95
	u’	902.3	+3	5958.83
	u”	907.4	+4	15515.97
	u”’	916.3	+4	37981.32
	v	881.9	+4	40056.95
	v_o	879.9	+3	3969.42
	v’	883.9	+3	31986.63

	v”	888.4	+4	45402.89
	v”’	897.9	+4	38152.57

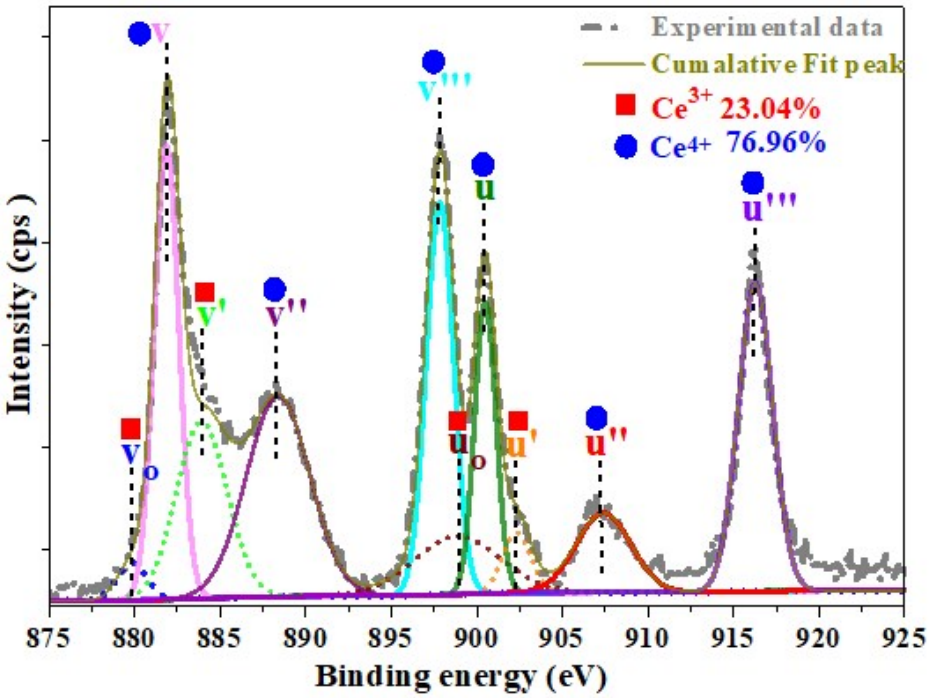

Fig. S1 Deconvoluted XPS spectra of Ce (3d) region

1.3 Optimization of Assay Conditions:

To ensure highest catalytic activity of CeO_2 NCs, influence of several parameters on experimental performance were investigated (Fig. S2, S3, S4, S7, S8 and S9).

It can be seen in Fig. S2 the catalytic reaction rate at pH 4.5 was found to be maximum for 0.3 mM TMB and 3.5 mM H_2O_2; same concentration of TMB and H_2O_2 was used at neutral pH to compare the catalytic potential. To examine the optimal incubation time under acidic (pH 4.5) and neutral (pH 7.4) condition, after every 180 seconds (sec.) we examine the catalytic capability at 652 nm. Fig. S7 shows for first 900 sec. the absorbance increases; later after 900 sec. shows no significant increase. Absorbance at 652 nm suggests the degree of reaction from TMB to oxTMB, and its intensity shows the catalytic ability. CeO_2 NCs shows the best catalytic activity after 900 sec. of reaction time. So, we selected an incubation period of 900 sec. for all the experiments at both the pH.

Further to establish a correlation between the increased POD-like activity of CeO_2 NCs (at neutral pH) and concentration of ATP, we examine the catalytic activity as a function of ATP concentration (ranging from 0.1 mM to 1.5 mM). As expected, increase in concentration of ATP observed a progressive increase in absorbance at 652 nm (Fig. S9(a)) and the highest catalytic activity observed at 1.5 mM concentration of ATP, demonstrating that the activity of

CeO_2 NCs can be tuned by controlling the ATP concentration. Similar study was performed with other adenosine analogues (ADP, AMP) and histidine; evidently ATP shows an augmented POD-like activity in CeO_2 NCs at neutral pH and catalytic order agrees to ATP > Histidine ≥ ADP >AMP, Fig. S9(a).

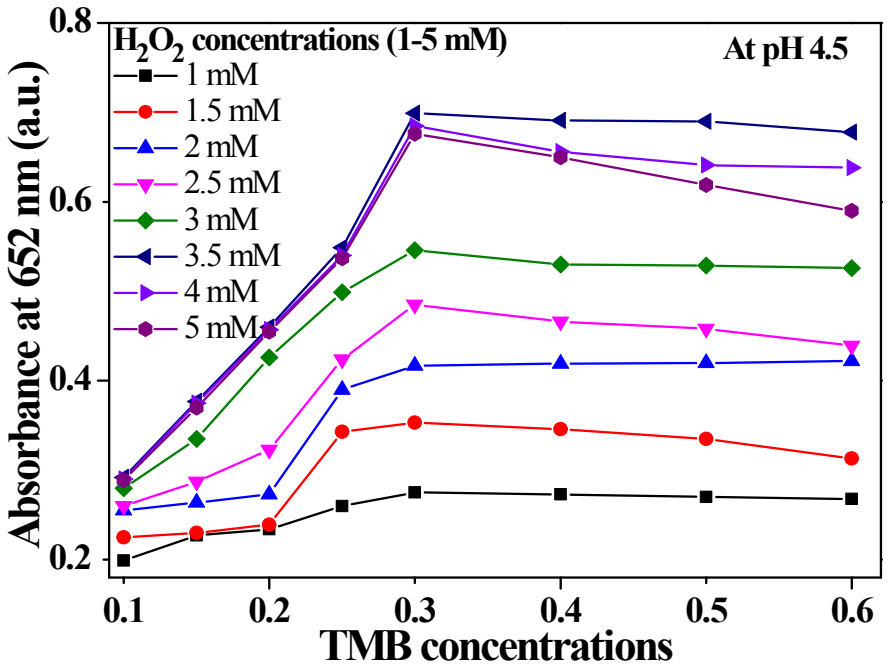

Fig. S2 Optimization of substrate (TMB & H_2O_2) concentration for POD-like-activity in CeO_2 NCs. at pH 4.5.

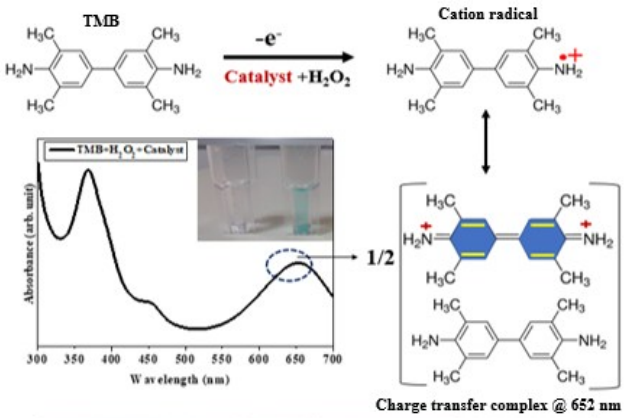

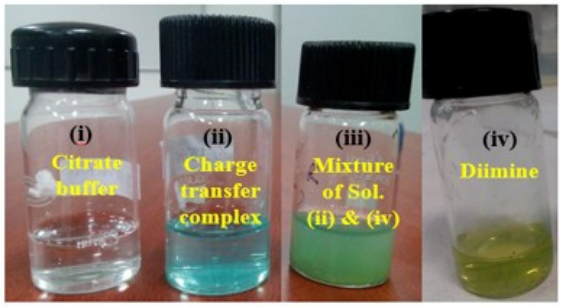

Fig. S3 Schematic illustration of catalyst (CeO_2 NCs.)-catalyzed oxidation of TMB and typical photography of TMB-H_2O_2 reaction system (i) with buffer only; (ii) Blue charge-transfer complex; (iii) Mixture of solution (ii)&(iv), (iv) Yellow Diimine.

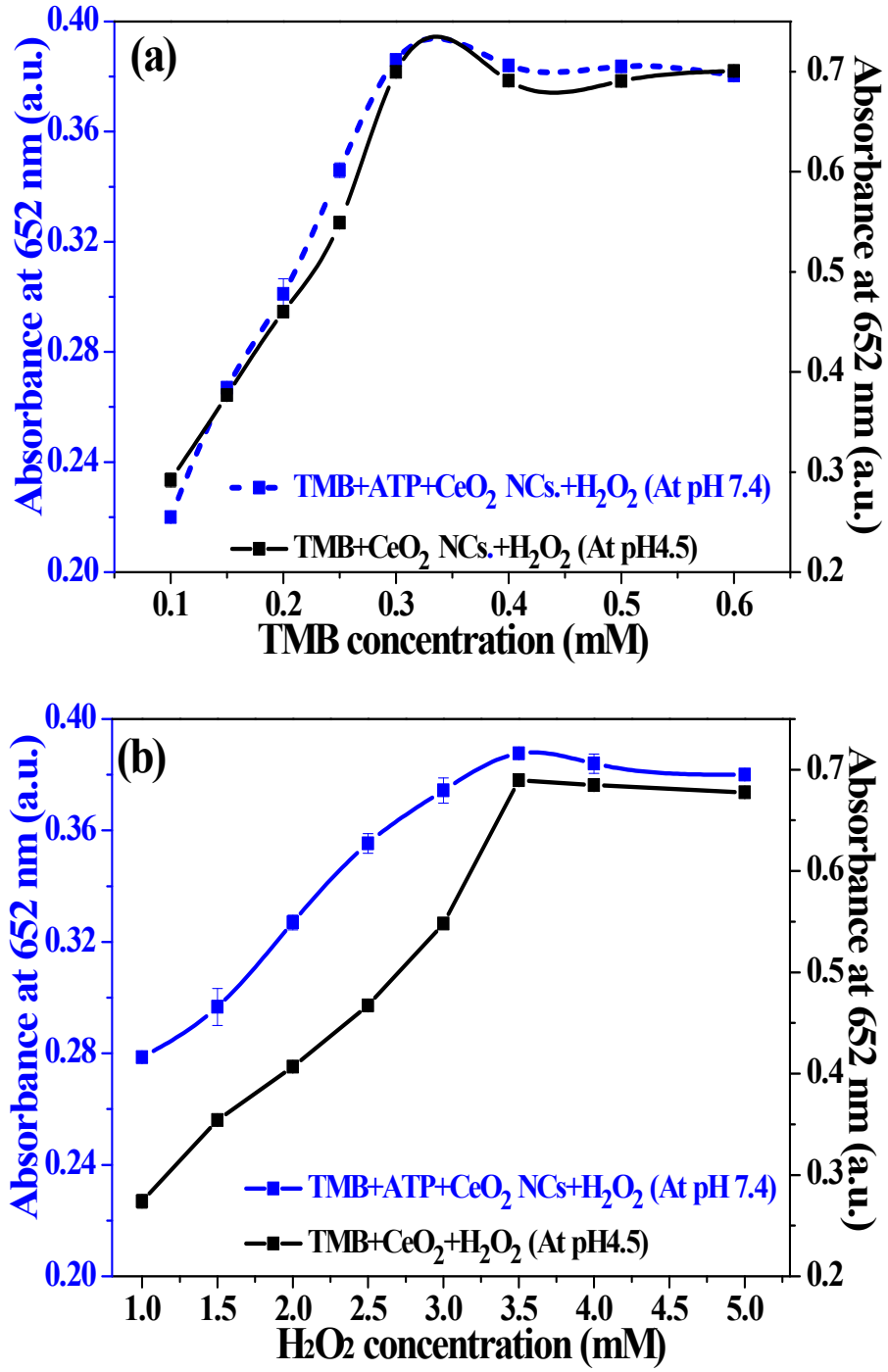

Fig. S4 Substrate concentration dependent POD-like activity of CeO_2 NCs. at pH 4.5 & 7.4 for **(a)** TMB 0.1-0.6 mM; **(b)** H_2O_2 1-5 mM.

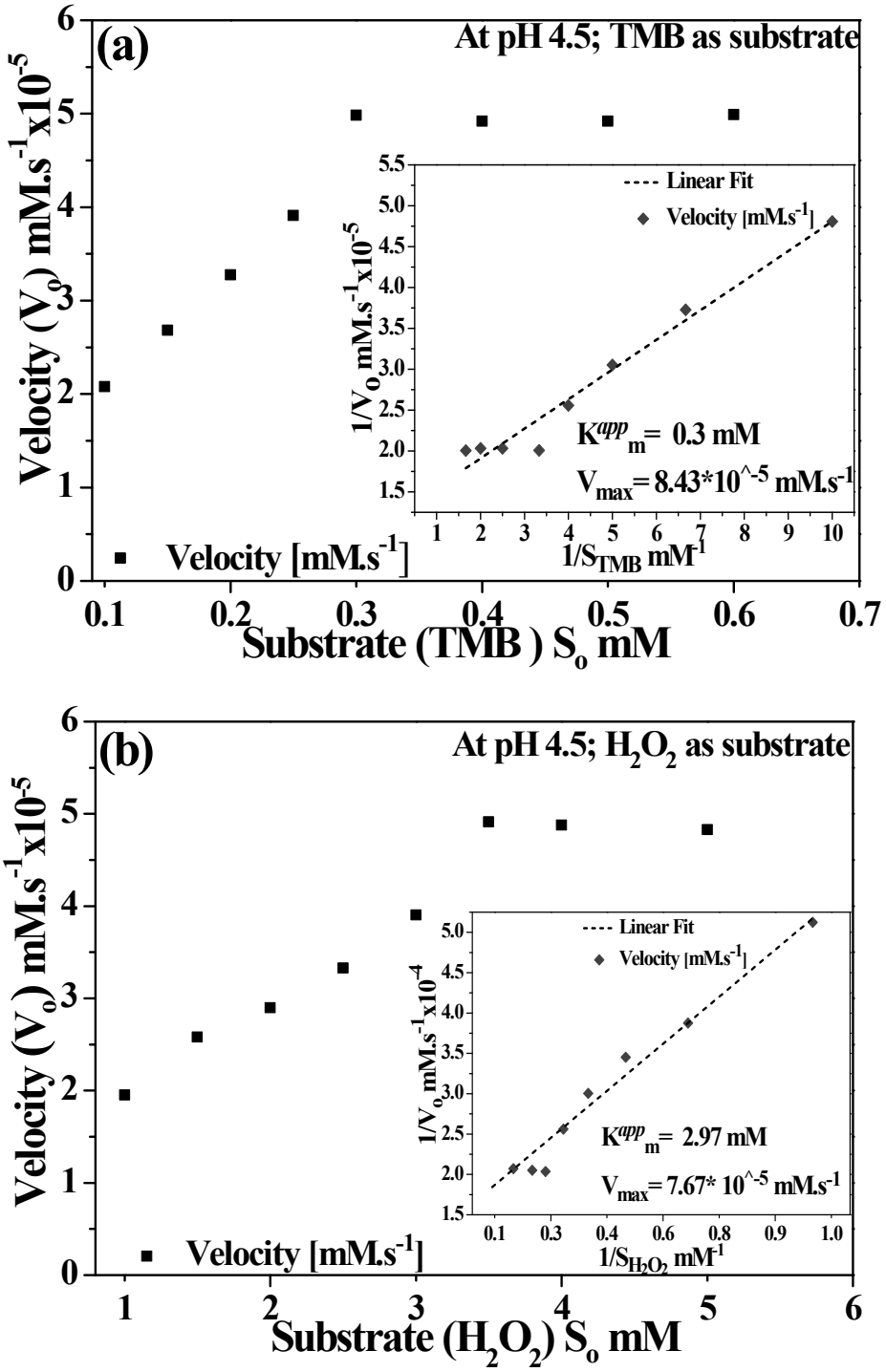

Fig. S5 Steady-state kinetic assay of CeO_2 NCs. at pH 4.5 **(a)** 3.5 mM of H_2O_2 with different concentrations of TMB (0.1-0.6 mM); **(b)** 0.3 mM of TMB mM with different concentrations of H_2O_2 (1-5 mM). Double reciprocal given as inset.

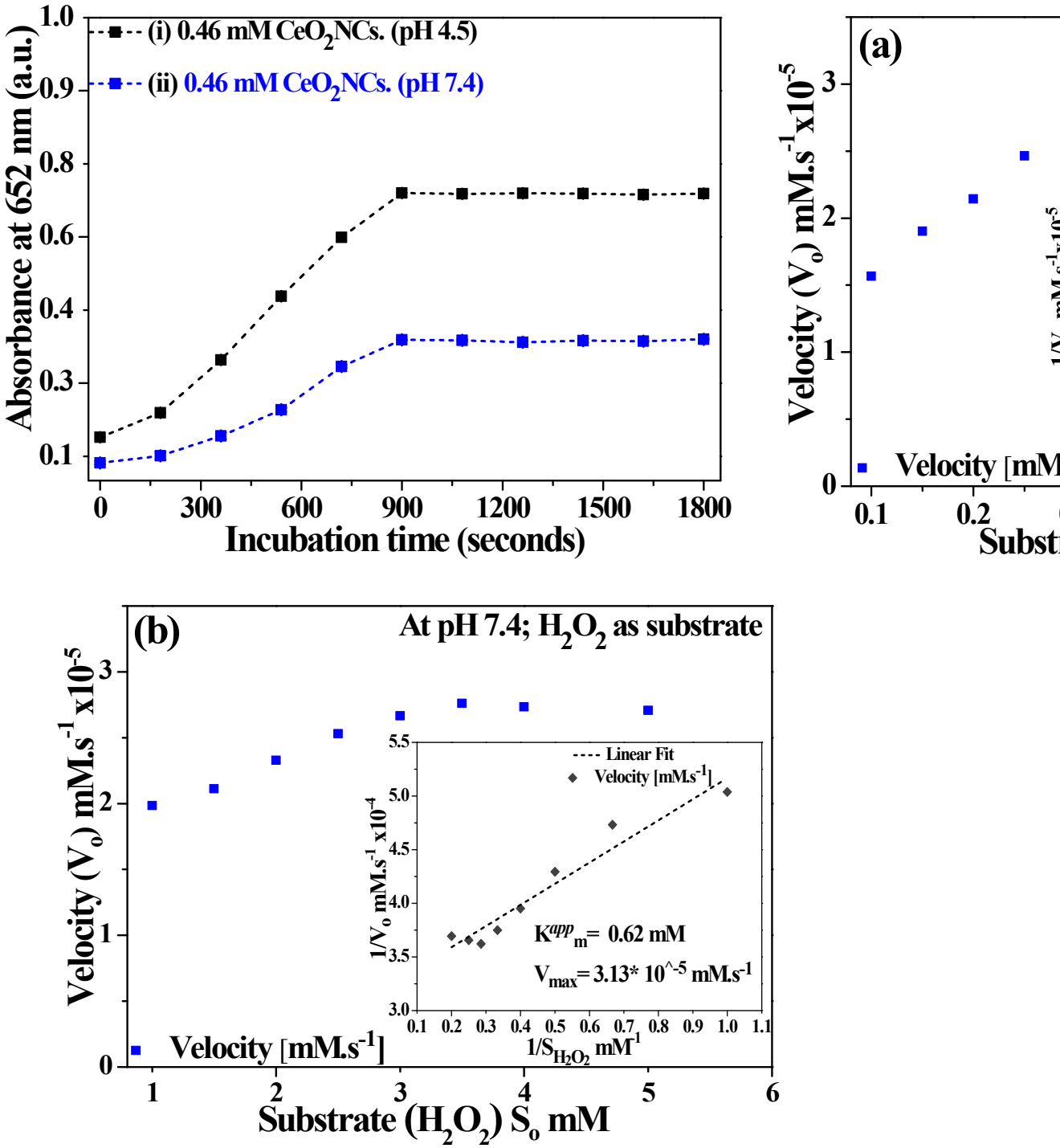

Fig. S6 Steady-state kinetic assay of CeO_2 NCs. at pH 7.4 **(a)** 3.5 mM of H_2O_2 with different concentrations of TMB (0.1-0.6 mM); **(b)** 0.3 mM of TMB mM with different concentrations of H_2O_2 (1-5 mM). Double reciprocal given as inset.

Fig. S7 Effect of incubation time on the absorbance of TMB-H_2O_2 reaction catalysed by CeO_2 NCs. at (i) pH 4.5 in citrate buffer; (ii) pH 7.4 in PBS. The concentrations of CeO_2 NCs., ATP, H_2O_2 and TMB are 0.46 mM, 1.5 mM, 3.5 mM and 0.3 mM respectively.

1.4. ATP ambits Catalyst POD activity to a broad pH range

Investigated catalyst (CeO_2 NCs.) POD activity by the oxidation of TMB in buffer solutions maintained at different pH values (3-10). Catalytic activity characterized by deep blue color solution, recorded absorbance at 652 nm after 15 min. of reaction at room temperature for four groups: (i) ATP+TMB+H_2O_2; (ii) TMB+CeO_2 NCs.+H_2O_2; (iii) TMB+ATP+CeO_2 NCs.+H_2O_2 and (iv) HRP+TMB+H_2O_2. Reactants optimum concentration acquired through a pre-optimization experiment, ESS 1.3.

We found group (i) shows a very weak absorption signal (Fig. S8a (i)) indicate no contribution towards POD-like-activity of the catalyst at all pH. This rules-out self-promoted activity of ATP while group (ii) clearly suggest catalyst POD-like activity is critical to pH. It was found catalysts at excessive low pH (below 4) shows a steep decline in the reaction, possibly indicates protonation of both the amino group of TMB leads to insusceptibility towards catalytic oxidation. Studies reported on aromatic amines under acidic medium (pH 2.5-3.5) have shown compromised sensitivity and product stability [2]. Catalyst POD reaction rises gradually (from pH 3.5) with optimal reaction at pH 4.5 evocative of an acid dependent reactivity on account of protonation in one of amino group in TMB and further the reaction declines with increase in pH; precisely after pH 6.5 insignificant POD reaction noted. The apparent decrease in the efficiency of colored product at alkaline pH implies an impeded electron transfer process due to H_2O_2 instability and its rapid decomposition into H_2O and O_2 [3]. Compared with group (iv),

optimal pH for POD reaction found to be identical for CeO_2 nanozyme and HRP. As known, activity of HRP strongly influenced by pH (Fig. S8a (iv)) this features similarity of CeO_2 NCs as POD mimic with natural equivalent for 'pH limitation' as prime factor that controls catalytic activity. Catalyst POD reaction at pH 4.5 operates ~1.25-fold high over natural enzyme i.e. HRP. Subsequent experiments with catalyst in acidic condition performed at pH 4.5.

In pursuit to emulate POD reaction at physiological condition (at pH 7.4). We introduced catalytic modulator 'ATP' to CeO_2+TMB+H_2O_2 system. It can be seen, catalyst POD reaction in presence of ATP shows a steady increase over a broad range of pH, Fig. S8a (iii). ATP found to improve catalyst POD activity ~20 times at pH 7.4. Here we presumed ATP imitates distal histidine residue of HRP which triggers H_2O_2 molecules available on Ce^{+3}/Ce^{+4} sites for •OH radical production, thus realizes catalyst POD feasibility at neutral pH.

Relative activity (%) summarized as heat map (Fig. S8 (b)) classified into four groups shown in different color schemes: maximum (green: ≥75%), moderate (blue: 50-74%), moderately low (light gold: 25-49%) and minimum (pink: 0-24%). The highest point specified as 100% relative activity. It reveals relative activity in group (iii) i.e.TMB+ATP+CeO_2 NCs.+H_2O_2 shows no activity below 24% and observes the maximum activity at pH 7.4, identifies ATP synergistic role for catalyst POD reaction at neutral pH; while relative activity in both group (ii) TMB+CeO_2 NCs.+H_2O_2 and group (iv) HRP+TMB+H_2O_2 demonstrates POD reaction in a narrow pH range. This underscore ATP stimulated catalyst POD execution over broad pH scope.

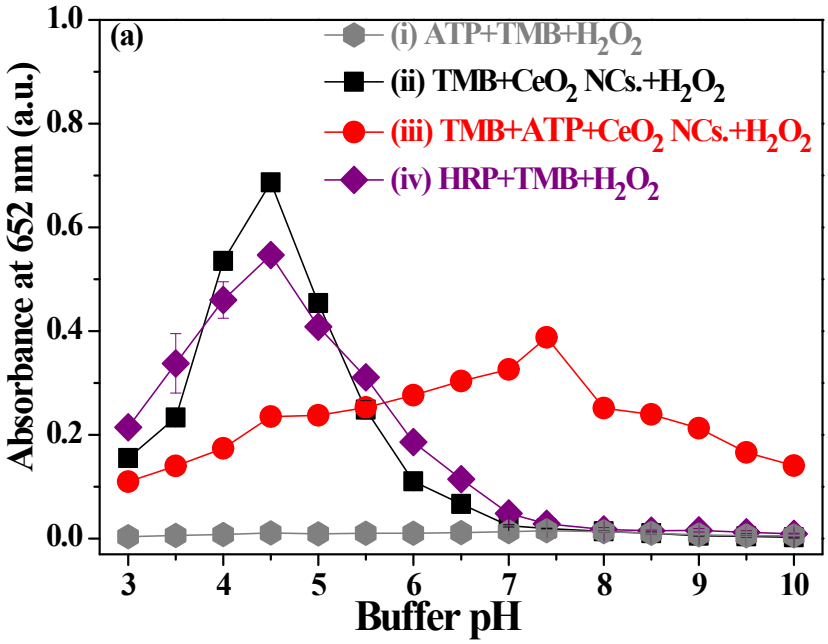

pH	HRP	(-) ATP	(+) ATP

(b)

3	39.27	22.6	28.35
3.5	61.74	33.96	36.16
4	84.09	77.87	44.92
4.5	100	100	60.74
5	74.76	66.08	61.34
5.5	56.89	36.2	65.2
6	34.03	16.06	71.3
6.5	21.03	9.7	78.34
7	8.96	3.63	84.02
7.4	5.22	2.86	100
8	3.22	2.03	64.85
8.5	2.8	1.55	61.76
9	2.98	0.87	54.8
9.5	2.31	0.68	42.86
10	1.76	0.38	36.25

Scale bar
≥ 75 %
50-74 %
25-49 %
0-24 %

Fig. S8 (a) Influence of pH on formation of oxidised TMB. Comparative performance of CeO_2 NCs. (0.46 mM) with HRP ($2.2*10^{-11}$ M); **(b)** Heat map for pH dependent relative activity (%). Reaction conditions at different pH (3-10) includes 1.5 mM, 3.5 mM and 0.3 mM concentrations of ATP, H_2O_2 and TMB respectively.

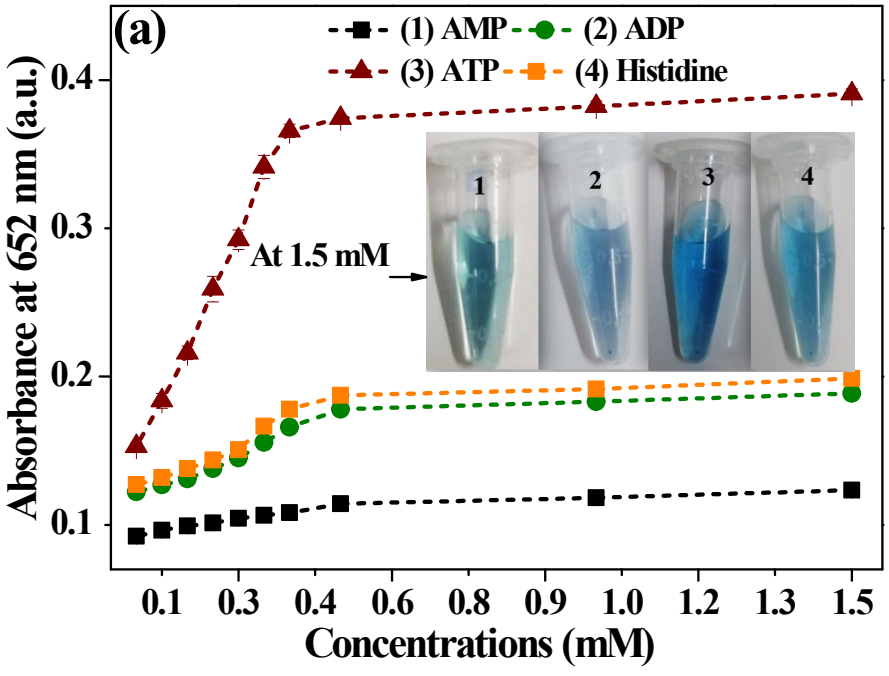

Fig. S9(a) Effect of adenosine analogues (AMP, ADP and ATP) and histidine on the TMB-H_2O_2 reaction catalysed by CeO_2 NCs. in PBS (1X) at pH 7.4.

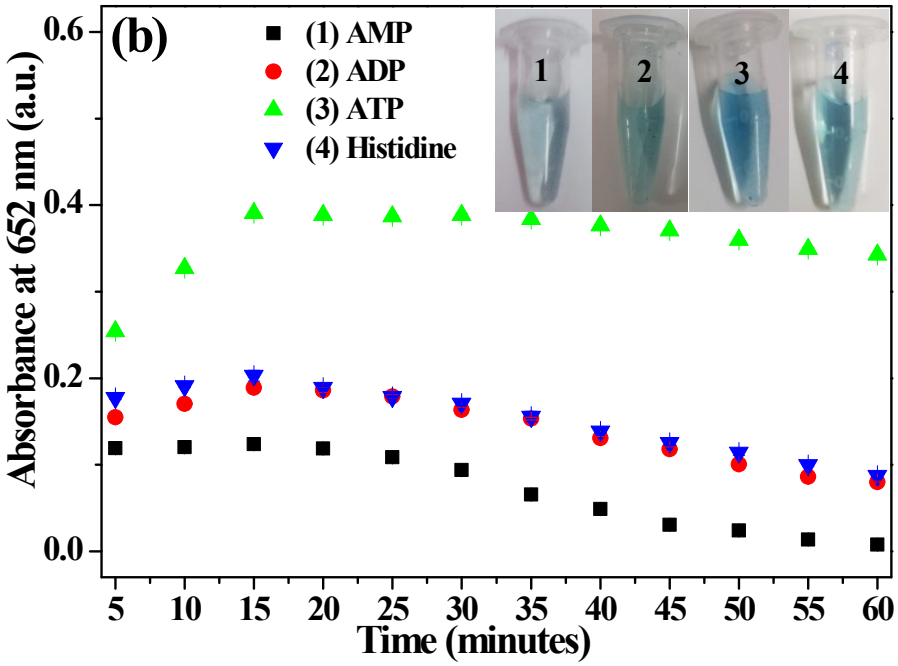

Fig. S9(b) Effect of adenosine analogues (AMP, ADP, ATP) and histidine in stabilizing cation radical ($TMB^{\cdot+}$) at neutral pH (7.4); inset shows the related color reactions after 60 minutes.

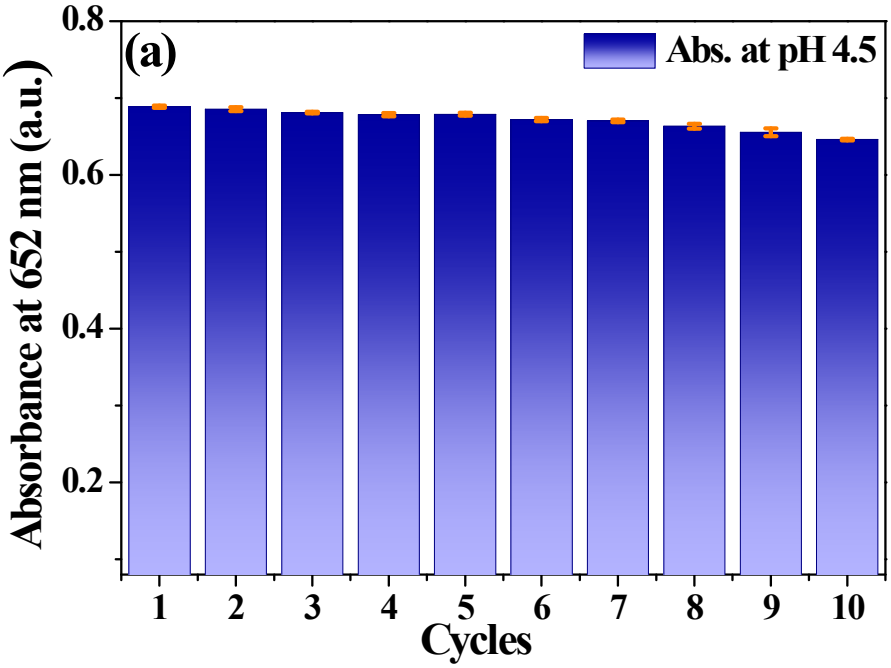

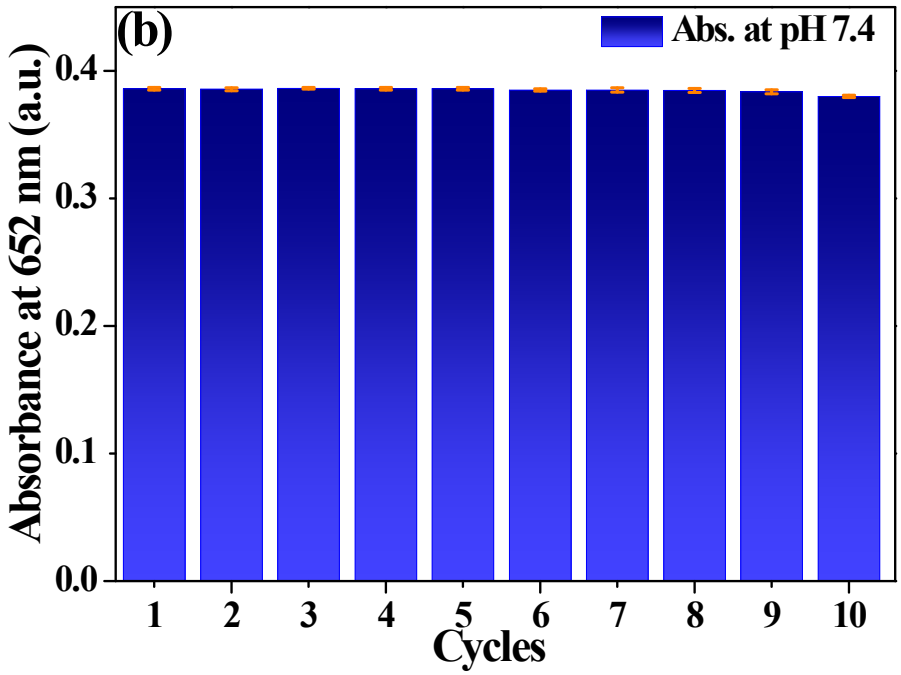

Fig. S10 Reusability Experiment: POD-like-activity in CeO_2 NCs. after every cycle at (a) pH 4.5; (b) pH 7.4.

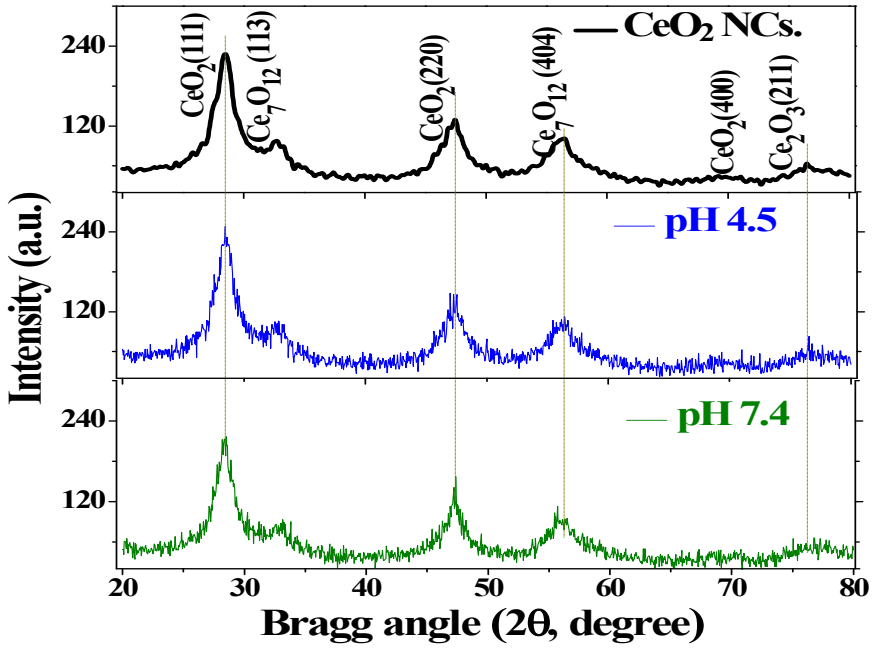

Fig. S11 XRD pattern of CeO_2 NCs. post synthesis and recovered after 10 catalytic cycles performed at pH 4.5 and 7.4.

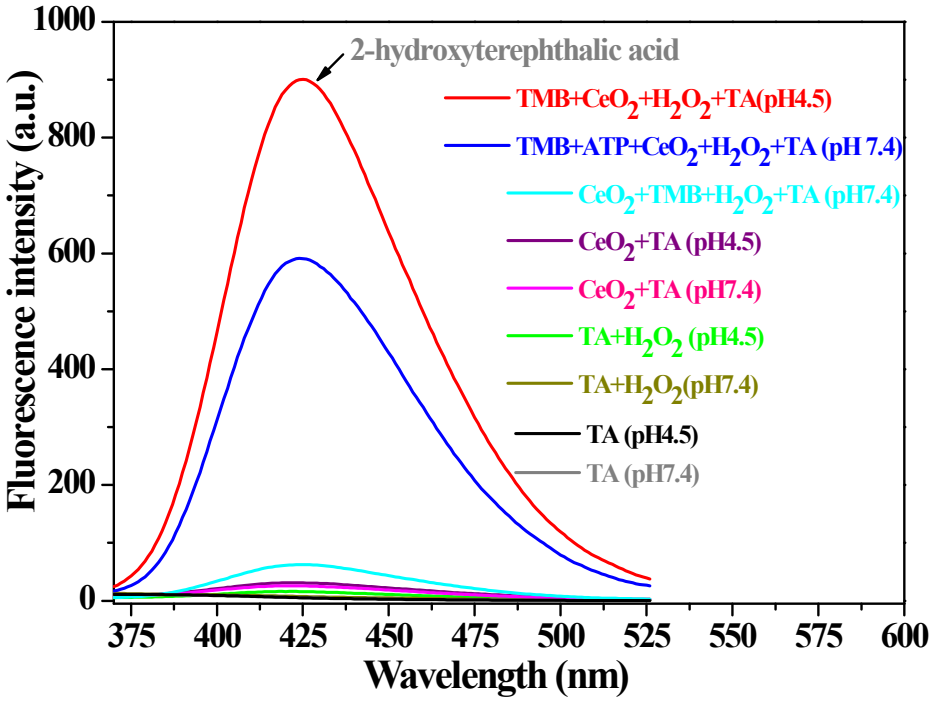

Fig. S12 Fluorescence spectra of 2- hydroxy terephthalic acid for detection of hydroxyl radical (•OH) using terephthalic acid (TA) as probe

1.5 Fluorometric Resazurin Microplate assay (f-REMA)

Anti-bacterial activity of catalyst alone and in combination was studied using resazurin (7-Hydroxy-3H-phenoxazin-3-one 10-oxide) reduction assay, recorded as mean fluorescence values for two bacterial species, Gram-positive (*S. aureus*) and Gram-negative (*E. coli*) at pH 4.5 and 7.4. This method overcome solubility issues of test materials and evaluated both fluorometrically and visually [4]. Chemical reduction based on cell metabolism monitored for irreversible reduction of resazurin into highly fluorescent pink color substance 'resorufin', indicates presence of metabolic activity/growth while non-fluorescent blue color interpreted as absence of metabolic activity/bacterial cell death.

Preliminary to f-REMA, calibration curves constructed for both the bacterial species to correlate bacterial cell concentration (CFU mL^{-1}) with resorufin fluorescence intensity (RFI), Fig. S13 (a & b). Using two and tenfold dilution bacterial suspension prepared to 0.001, 0.005, 0.01, 0.05, 0.1, 0.5 and $1*10^5$ CFU mL^{-1}. An optimization experiment on resazurin metabolization finds 0.002 % (20 µL) reduction in 35 min. used in the present study to record stable resorufin fluorescence in both the test isolates. f-REMA carried out to monitor reduction

in resorufin RFI for test samples (NCs/H_2O_2/ATP) alone or in combination with bacterial culture + redox dye, growth medium with redox dye as positive control and bacterial culture in growth medium with redox dye (without NCs/H_2O_2/ATP) as negative control. Fluorometric measurement carried out at excitation/ emission wavelength of 530 nm/ 580 nm for 180 minutes.

Curve fitting analysis on bacterial cell density verses resorufin fluorescence were made in Origin Pro 8.5. Linear regression equation (i) and correlation coefficient quotient (R^2) estimated for both the bacterial isolates. Calibration curve derived average bacterial number, represented as log (CFU mL^{-1}± SD) where n=3 verses were used to calculate % bacterial inhibition using equation (ii), [5].

$$FI\ (resorufin)\ = slope * \ (CFU\ mL - 1)\ +\ intercept \qquad \text{(i)}$$

$$\%\ Bacteria\ Inhibtion = 100 - (Log\frac{(S_{180\ min.})}{(C_{\ -\ ve\ 180\ min.})} * 100) \qquad \text{(ii)}$$

Where, $S_{180\ min.}$= Logarithm of average bacterial cells (CFU mL^{-1}) in treated group after 180 min.; $C_{\text{-ve}180\ min.}$= Logarithm of average bacterial cells (CFU mL^{-1}) in untreated group (negative control) after 180 min.

1.6 Minimum Inhibitory Concentration (MIC):

Broth microdilution was performed following Clinical and Laboratory Standards Institute (CLSI) guidelines with some modification, coupling redox indicator 'resazurin' to distinguish metabolically viable cells from non-viable cells [6]. Prior to MIC experiment, to eliminate false positive results it was ensured that the catalyst (CeO_2), ATP and H_2O_2 do not interfere with redox dye at both the pH (4.5 and 7.4). This was considered as positive control and negative control includes medium + bacterial culture + redox dye.

MIC_{99} was determined against both the bacterial cells (*S. aureus* and *E. coli*) with a final cell density corresponds to $1*10^5$ CFU mL^{-1} for (a) CeO_2 NCs, (b) H_2O_2, (a)+(b) and (a)+(b) +ATP at pH 4.5 and 7.4. Followed an incubation of 18 hrs. added redox indicator (20 µL; 0.002%) to all wells and observed for color change after 2.5 hrs. Number of viable cells is directly proportion to the intensity of color produced. Lowest concentration prior to color change was considered as MIC value where cells losses its metabolic potential to reduce resazurin (blue) into resorufin (pink fluorescent dye).

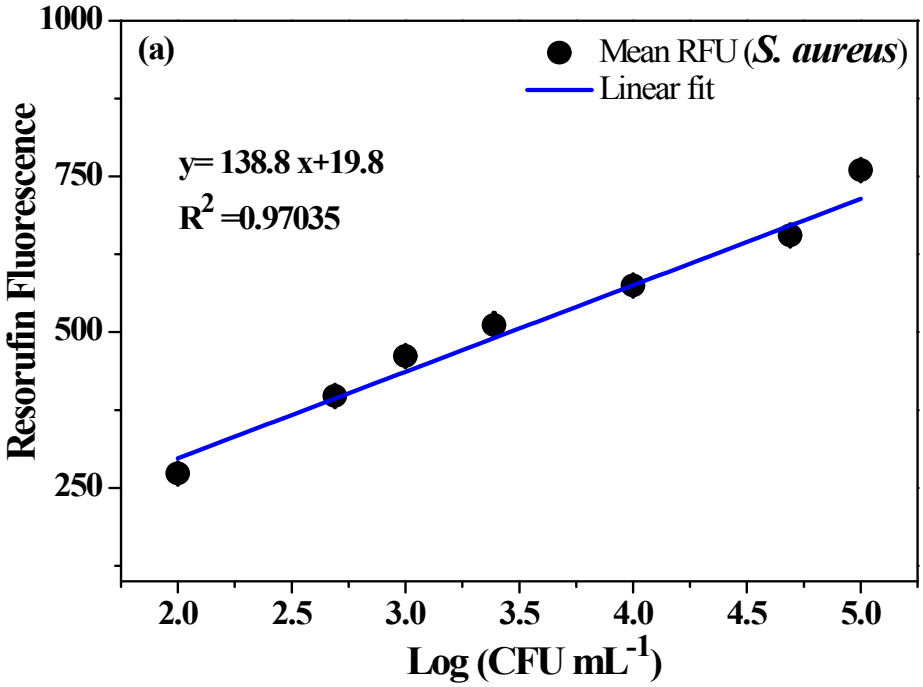

Fig. S13 (a) Calibration curve for *S. aureus*

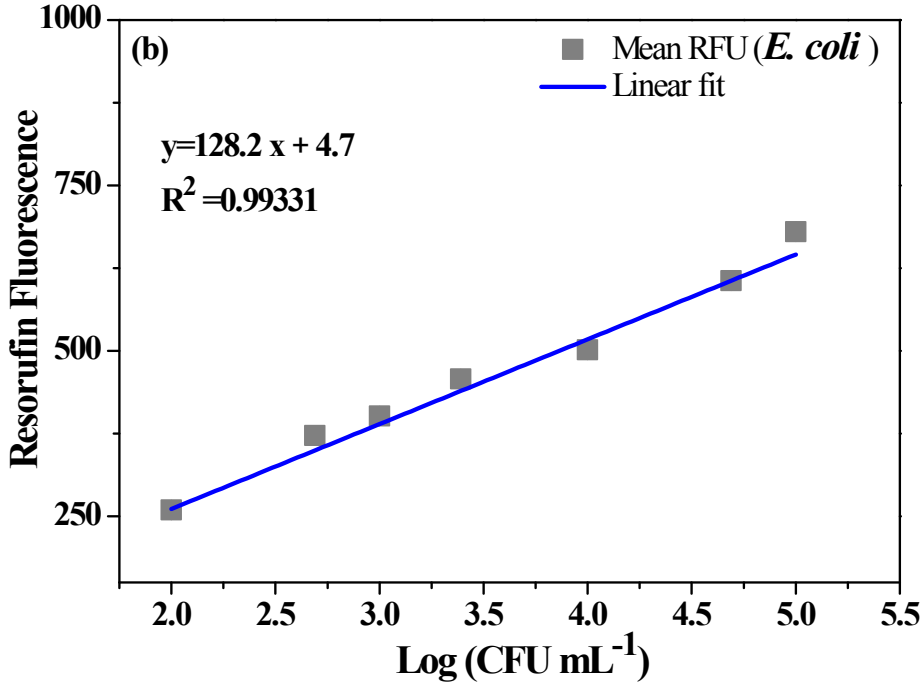

Fig. S13 (b) Calibration curve for *E. coli*

Table S2 Catalyst $MIC_{99\%}$ (μg mL^{-1}) alone and in combination:

Test compound	pH 4.5		pH 7.4	
	S. aureus	*E. coli*	*S. aureus*	*E. coli*
CeO_2 NCs	250	186.7	225	200
H_2O_2[a]	5	4	7.5	5.5
CeO_2 NCs+ H_2O_2	108	50	216	170
CeO_2 NCs+H_2O_2+ATP	100	47	115	78

Note: MIC values corresponds to minimum 3 concordant values collected from 3-6 replicates
a: concentration in mM

1.7 Influence of H_2O_2 on bacterial growth (at pH 4.5 & 7.4):

To exhibit CeO_2 nanozyme POD approach in suppressing bacterial growth *in vitro*, we optimize the concentration of H_2O_2 that shows bactericidal effect. Investigated the effect of oxidant (H_2O_2) at different concentrations (1, 2.5, 3.5 and 5 mM) against Gram-positive (*S. aureus*) and Gram-negative (*E. coli*) bacterial cells at pH 4.5 and 7.4.

Fig. S14 (a) shows the (%) bacterial survival as a function of oxidant concentrations. At both the pH a concentration dependent effect observed, *E. coli* being more susceptible over *S. aureus.* This well accords to MIC_{99} values given in Table S2. Further the oxidant exposed cells were quantified for malondialdehyde–thiobarbituric acid (MDA–TBA) adduct using the standard calibration curve (Y= 0.06848X+ 0.07535), given in inset of Fig. 14 (b). As a measure of H_2O_2 induced oxidative damage incurred in bacterial membrane, Lipid peroxidation was estimated [7]. It was found exposure of 3.5 mM and 5 mM of H_2O_2 reveals maximum MDA equivalents in *E. coli* over *S. aureus* at both the pH, Fig. S14 (b). It is seen clearly, H_2O_2 exposure at 5mM reveals an effective bacterial growth inhibition at both the pH..

Through a substrate (H_2O_2) optimization experiment at pH 4.5 and 7.4, it was found catalyst gave optimal POD reaction at 3.5 mM H_2O_2 concentration (Fig. 14 (c)), further increase in H_2O_2 concentration causes decline in POD activity. This might possibly be due to decrease in

Ce^{3+} species and excess H_2O_2 concentration disrupts $Ce^{4+} \rightarrow Ce^{3+}$ transitions and obstruct •OH generation potential at both the pH, inset Fig. 14 (c).

Consequently, all anti-bacterial study performed at 3.5 mM concentration of oxidant (H_2O_2). This does not impede catalyst regeneration ability, catalyse conversion of H_2O_2 into •OH radical mediated bacterial killing.

Our finding reinforces CeO_2 nanorods anti-bacterial (in acidic and neutral pH) effect without any external irradiation source. Catalyst excellent POD activity at pH 4.5 foresees application to eradicate pathogenic microflora in dental regime. Achieving POD feasibility at physiological pH open doors to a variety of biological applications.

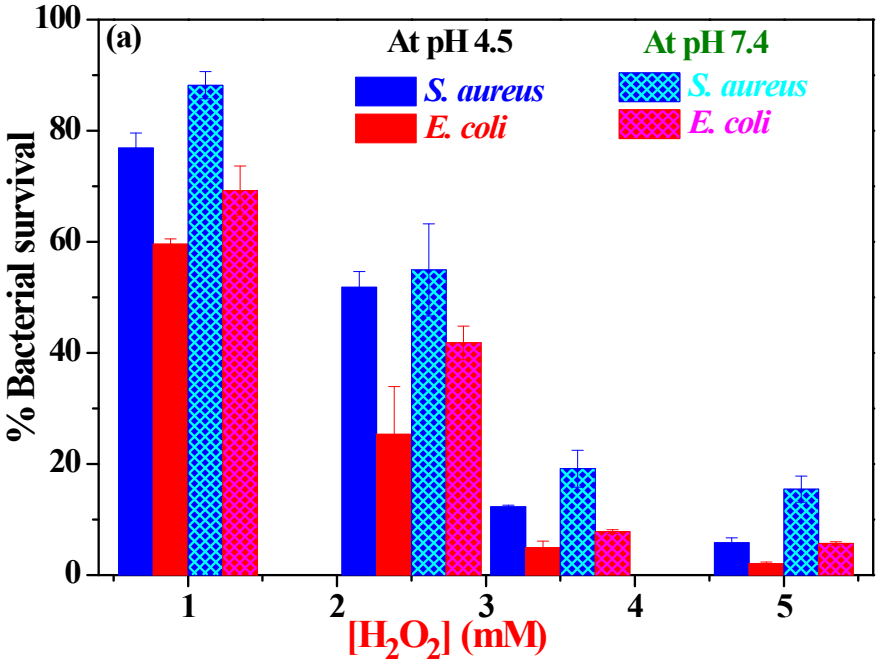

Fig. 14 (a) Bacterial Survival (%) verses oxidant (H_2O_2) concentrations at pH 4.5 and 7.5.

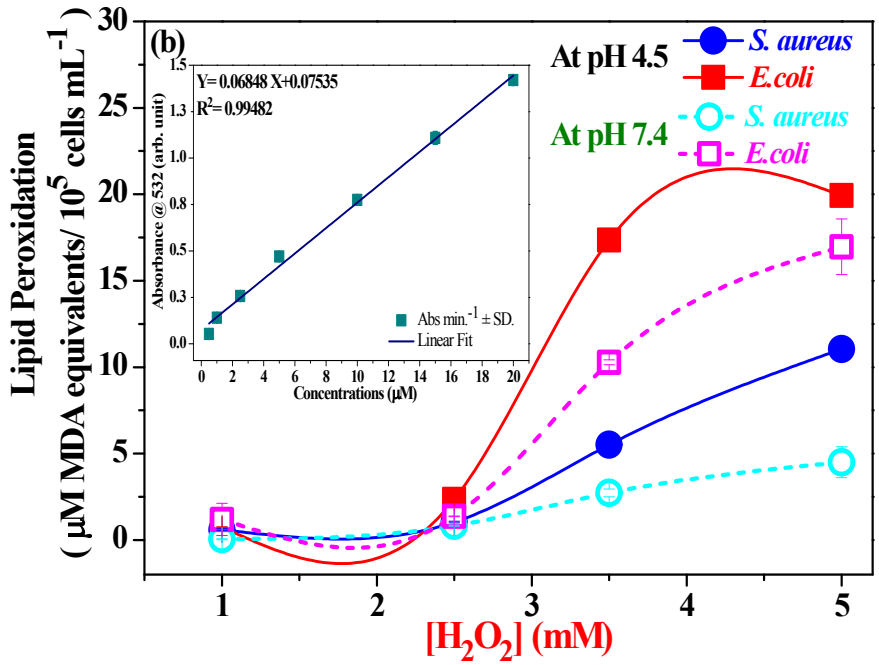

Fig. 14 (b) Lipid Peroxidation in oxidant (H_2O_2) treated bacterial cells at pH 4.5 and 7.5.

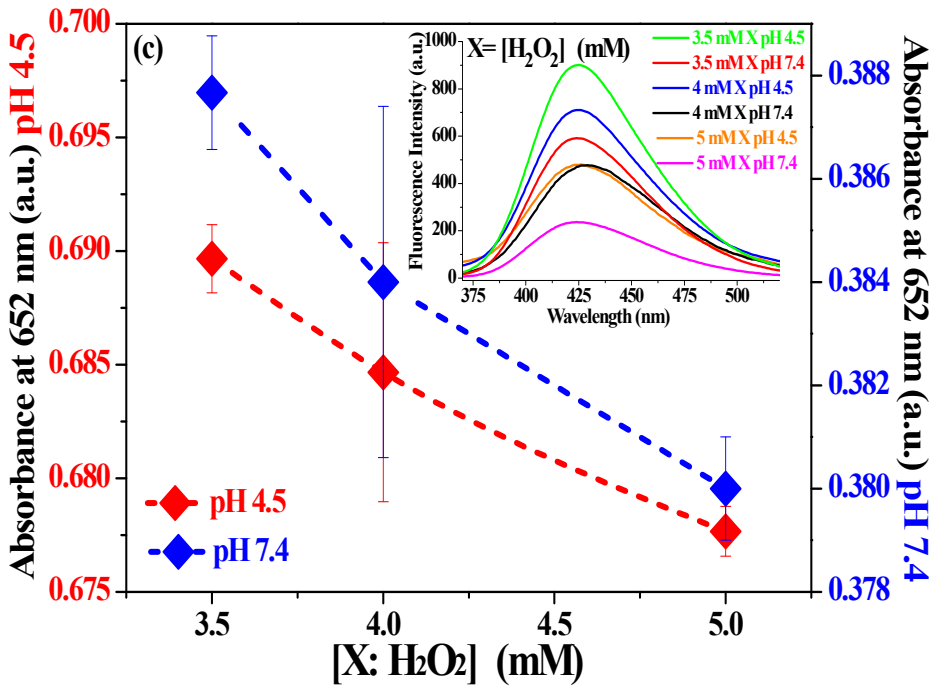

Fig. 14 (c) Catalyst substrate (H_2O_2) dependent POD activity, inset shows •OH radical generation using TA probe at pH 4.5 and 7.5.

Table S3 Comparative Assessment of CeO_2 NCs. Anti-bacterial potential with earlier reports:

Salt precursor, Synthesis method & Nanoproduct	Shape & Average Size (nm)	Microbiological technique, pH & Concentration	Test organism		Mode of action	Ref. & Year
			S. aureus	*E. coli*		
(NH_4) $Ce(NO_3)_6$; microwave assisted ; CeO_2	Spherical [a](~45 nm)	Agar diffusion	5 mm	7 mm	NPs absorption on bacterial cell wall	[8] 2016
$CeCl_3.7H_2O$; hydrothermal; CeO_2	honeycomb	Agar diffusion (at 100 mg)	24 mm	26 mm	Photogeneration of ROS, electrostatic bond between NPs. and bacterial cell membrane.	[9] 2019
$Ce(NO_3)_3.6H_2O$; hydrothermal; CeO_2	Cube and octahedral	Agar diffusion	25 mm	22 mm	CeO_2 NPs. oxygen vacancies	[10] 2019
$Ce(NO_3)_3.6H_2O$; Green synthesis; CeO_2	Cube	Agar diffusion	9 mm	No inhibition	-	[11] 2019
$Ce(NO_3)_3.6H_2O$; Green synthesis; chitosan-CeO_2	Spherical [b](23.12-89.91 nm)	Agar diffusion	-	11 mm	Direct interaction of NPs-bacterial cell wall causes membrane disruption	[12] 2017

$Ce(NO_3)_3.6H_2O$; hydrothermal; CeO_2	-	Agar diffusion	-	0 mm	-	[13] 2013
		MIC (mg mL^{-1}) pH 7.4		3		
$Ce(NO_3)_3.6H_2O$; Sol-gel; CeO_2	[a](~4.2 nm)	Log (CFU mL^{-1}) at 1 mM -24 hrs.	1.53±0.07	1.11±0.02	-	[14] 2012
$CeCl_3.7H_2O$; Coprecipitation; CeO_2	Nanorods Mean length (nm) [a](197±13.4) [b](214±6.4)	**At pH 4.5 -3hrs** Log (CFUmL^{-1}); (MIC µg mL^{-1}) **CeO_2**	4.25±0.47 (250)	2.90±0.19 (186.7)	CeO_2 NCs POD mimic based •OH radical enabled bacterial growth reduction at pH 4.5	**Present work**
		CeO_2+H_2O_2	1.47±0.18 (108)	0.82±0.28 (50)		
		CeO_2+H_2O_2 +ATP	1.27±0.14 (100)	0.63±0.31 (47)		
		At pH 7.4 -3hrs Log (CFUmL^{-1}); (MIC µg mL^{-1}) **CeO_2**	3.43±0.07 (225)	3.18±0.25 (200)	ATP facilitate POD mimic CeO_2 NCs. for •OH radical mediated bacterial reduction at pH 7.4.	
		CeO_2+H_2O_2	3.03±0.01 (216)	2.77±0.03 (170)		
		CeO_2+H_2O_2 +ATP	1.41±0.02 (115)	1 ±0.11 (78)		

Note: MIC: Minimum Inhibitory Concentration; POD: Peroxidase; a: TEM; b: FE-SEM; (-) Not reported

References

[1] R. Asuvathramana, K.I. Gnanasekara , P.C. Clinsha , T.R. Ravindran and K.V. Govindan Kutty, Investigations on the charge compensation on Ca and U substitution in $CePO_4$ by using XPS, XRD and Raman spectroscopy, *Ceramics International*, 2015, **41**, 3731-3739.

[2] M. Drozd, M. Pietrzak, P. G. Parzuchowski and E. Malinowska, Pitfalls and capabilities of various hydrogen donors in evaluation of peroxidase-like activity of gold nanoparticles, *Anal Bioanal Chem*., 2016, **408**, 8505–8513.

[3] C. L. Hsueh, Y. H. Huang, C. C. Wang and C. Y. Chen, Degradation of azo dyes using low iron concentration of Fenton and Fenton-like system, *Chemosphere*, 2005, 58, 1409-1414.

[4] C. Pardo-Castano, D. Vasquez, G. Bolanos and A. Contreras, Strong antimicrobial activity of collinin and isocollinin against periodontal and superinfectant pathogens in vitro, *Anaerobe*,2020, **62**, 102163.

[5] O. Tyc, L. Toma´s-Menor, P. Garbeva, E. Barrajon-Catalan and V. Micol, Validation of the Alamar Blue Assay as a Fast Screening Method to Determine the Antimicrobial Activity of Botanical Extracts, *PLoS ONE*, 2016, **11**, e0169090.

[6] Clinical and Laboratoy Standars Institute, Performance Standards for Antimicrobial Susceptibility Testing, CLSI Document M100-S25, Wayne, PA, 2015.

[7] S.R. Sarker, S. A. Polash, J. Boath, A. E. Kandjani, A. Poddar, C. Dekiwadia, R. Shukla, Y. Sabri and S.K. Bhargava, Functionalization of elongated tetrahexahedral Au nanoparticles and their antimicrobial activity assay, *ACS Appl. Mater. Interfaces*, 2019, **11**, 13450–13459.

[8] T.V. Surendra and S. M. Roopan, Photocatalytic and antibacterial properties of phytosynthesized of CeO_2 NPs using *Moringa oleifera* peel extract, *Journal of Photochemistry and Photobiology B: Biology*, 2016, **161**, 122-128.

[9] P. Nithya, M. Balaji, A. Mayakrishnan, C. Dhilip Kumar, S. Rajesh, A. Surya and M. Sundrarajan, Ionic liquid functionalized biogenic synthesis of Ag-Au bimetal doped CeO_2 nanoparticles from Justicia adhatoda for pharmaceutical applications: Antibacterial and

anti-cancer activities, *Journal of Photochemistry & Photobiology, B:* Biology,2019, **202,** 111706.

[10] A. Balamurugan, M. Sudha, S. Surendhiran, R. Anandarasu, S. Ravikumar, Y.A. Syed Khadar, Hydrothermal synthesis of samarium (Sm) doped cerium oxide (CeO_2), *Materials Today: Proceedings*, 2019, https://doi.org/10.1016/j.matpr.2019.08.217.

[11] S. Sebastiammal, A. Mariappan, K. Neyvasagam and A. Lesly Fathima, *Annona Muricata* Inspired Synthesis of CeO_2 Nanoparticles and their Antimicrobial Activity *Materials Today: Proceedings*, 2019, **9**, 627–632.

[12] R.P. Senthilkumar, V. Bhuvaneshwari, R. Ranjithkumar, S. Sathiyavimal, V.Malayaman and B. Chandarshekar, Synthesis, characterization and antibacterial activity of hybrid chitosan-cerium oxide nanoparticles- as a bionanomaterials, *International Journal of Biological Macromolecules*, 2017, **104**, 1746-1752.

[13] R. Cuahtecontzi-Delint, M. A. Mendez-Rojas, E. R. Bandala, M. A. Quiroz, S. Recillas, and J. Luis Sanchez-Salas, Enhanced Antibacterial Activity of CeO_2 Nanoparticles by Surfactants, *International Journal of Chemical Reactor Engineering* 2013, **11**, 781–785.

[14] L.P. Babenko, N.M. Zholobak, A.B. Shcherbakov, S.I.Voychuk, L.M. Lazarenko, and M.Ya. Spivak, Antibacterial activity of Cerium colloids against opportunistic microorganisms *in vitro*, *Mikrobiol Z*, 2012, **74**, 54-62.